# SYNTHESIS AND PHOTOCATALYTIC PROPERTIES OF CeVO$_4$ NANOPARTICLES UNDER UV IRRADIATION

P. INTAPHONG[a], S. JONJANA[b], A. PHURUANGRAT[b*], P. POOKMANEE[a], S. ARTKLA[c], S. THONGTEM[d], T. THONGTEM[e,f]

[a]*Department of Chemistry, Faculty of Science, Maejo University, Chiang Mai 50290, Thailand*
[b]*Department of Materials Science and Technology, Faculty of Science, Prince of Songkla University, Hat Yai, Songkhla 90112, Thailand*
[c]*Faculty of Art and Science, Roi-Et Rajabhat University, Selaphum, Roi-Et 45120, Thailand*
[d]*Department of Physics and Materials Science, Faculty of Science, Chiang Mai University, Chiang Mai 50200, Thailand*
[e]*Department of Chemistry, Faculty of Science, Chiang Mai University, Chiang Mai 50200, Thailand*
[f]*Materials Science Research Center, Faculty of Science, Chiang Mai University, Chiang Mai 50200, Thailand*

In this research, CeVO$_4$ nanoparticles have been successfully synthesized by hydrothermal reaction. The as-synthesized CeVO$_4$ nanoparticles were characterized by X-ray powder diffraction (XRD), Raman spectroscopy, Fourier transform infrared (FTIR) spectrophotometry and scanning electron microscopy (SEM). The photocatalytic activity of the as-synthesized CeVO$_4$ nanoparticles was evaluated via the photodegradation of methylene blue (MB) under UV irradiation. In this research, the tetragonal CeVO$_4$ nanoparticles with the particle size less than 100 nm were detected. The V–O stretching and bending in VO$_4^{3-}$ tetrahedrons were detected by FTIR and Raman spectrometry. The photocatalysis of MB by CeVO$_4$ nanoparticles exhibited the decolorization efficiency of 80 % within 300 min.

## 1. Introduction

In recent years, semiconductor photocatalysts such as TiO$_2$ and ZnO have been focused to solve environmental and energy problems: photocatalytic degradation, elimination of organic pollutants, H$_2$ evolution, etc [1–4]. Rare earth orthovanadates (LnVO$_4$, Ln = Ce, La, Nd, Gd) have been intensively studied for using as promising inorganic materials due to their potential applications in catalysts, laser host materials, magnetic materials, electrochromic materials, gas sensors and phosphors [5–7]. Zircon-type CeVO$_4$ is one of rare earth orthovanadates and important semiconducting derivatives due to their electronic and catalytic properties such as oxidative catalysts, gas sensors, luminescence materials, electrochromic materials and components for solid oxide fuel cells (SOFCs) [6–8].

Our motivation is to report the synthesis of CeVO$_4$ nanoparticles by hydrothermal method and to study its photocatalytic properties. The products were characterized by X-ray diffraction (XRD), scanning electron microscopy, Raman spectroscopy and Fourier transform infrared (FTIR) spectroscopy. The photocatalytic property was tested through methylene blue (MB) degradation

---

*Corresponding authors: phuruangrat@hotmail.com

under UV irradiation. The photocatalytic property of $CeVO_4$ exhibited 80 % MB degradation (5 x $10^{-5}$ M) by 0.05 g $CeVO_4$ nanoparticles.

## 2. Experiment

All chemicals were analytical grade and were used without further chemical treatment during the whole synthesis process. In a typical procedure, each of 5 mmol $Ce(NO_3)_2 \cdot 5H_2O$ and $Na_2VO_4$ was dissolved in each 100 ml RO water and mixed together. The obtained solutions were stirred and adjusted the pH to 1–4 by 3 M HCl solution. Each mixture was transferred to a 200 ml Teflon-lined stainless steel autoclave, tightly closed and maintained at 200 °C in an electric oven for 24 h. The obtained precipitates were washed with distilled water and ethanol, dried at 80 °C for 24 h, and collected for further characterization.

The phase of the as-synthesized products was characterized by X-ray diffraction with Cu $K_\alpha$ radiation (1.54056 Å) of a Philips X'Pert MPD X-ray diffractometer (XRD) operating at 30 kV with 0.02 $^\circ \cdot s^{-1}$ scanning rate. The morphology was characterized by scanning electron microscopy (SEM, JEOL JSM-6335F) using $LaB_6$ as an electron gun with 15 kV accelerating voltage. Raman spectrum was recorded on a HORIBA JOBIN YVON T64000 Raman spectrometer with 50 mW and 514.5 nm wavelength Ar green laser, and FTIR spectrum on a BRUKER TENSOR 27 Fourier transform infrared (FTIR) spectrometer with KBr as a diluting agent and operated in the range of 400–4,000 $cm^{-1}$.

The photocatalytic performance of the as-synthesized samples was evaluated through the photocatalytic degradation of methylene blue (MB) under UV light irradiation. The 0.05 g of $CeVO_4$ nanoparticles was dispersed in 200 ml containing 5 x $10^{-5}$ M MB solution. The mixed suspension was magnetically stirred for 30 min in the dark to reach an adsorption–desorption equilibrium. Under ambient conditions and stirring, the mixed suspension was exposed to UV irradiation. Every a certain time interval, 5 ml of the mixed suspension was collected and centrifuged to remove the photocatalyst for determining of MB concentration. The process was monitored by measuring the absorption of MB in the filtrate at 664 nm wavelength using a UV–visible spectrometer (Perkin Elmer Lambda 25 UV-VIS spectrometer). Decolorization efficiency (%) was calculated by the equation

$$\text{Decolorization efficiency (\%)} = \frac{C_o - C_t}{C_o} \times 100 \qquad (1)$$

where $C_o$ is the initial concentration of MB and $C_t$ is the concentration of MB after visible light irradiation for the elapsed time (t).

## 3. Results and discussion

X-ray diffraction patterns of the as-synthesized $CeVO_4$ products at pH 1–4 are shown in Fig. 1. The XRD pattern of $CeVO_4$ at the pH of 4 was specified as the mixed phases of orthorhombic $V_2O_5$ structure (JCPDS no. 09-0387) [9] as major phase and tetragonal $CeVO_4$ structure (JCPDS no. 79-1065) as minor phase. When the pH of the solution increased from 4 to 1, the XRD analysis showed that the orthorhombic $V_2O_5$ structure was decreased while tetragonal $CeVO_4$ structure was increased. Only tetragonal $CeVO_4$ nanostructure corresponding to the JCPDS no. 79-1065 [9] was synthesized at the pH of 1. There was no detection of other phases such as $CeO_2$ and $V_2O_5$. The Scherrer equation used for calculation of particle size (d) is given as follows

$$d = \frac{0.94\lambda}{\beta \cos\theta} \qquad (2)$$

, where $\lambda$ is the wavelength of the Cu $K_\alpha$ radiation (1.54056 Å), $\beta$ is full width at half maximum (FWHM) of the XRD peak, and $\theta$ is the diffraction angle of the corresponding peak [10, 11]. The calculated particle size of tetragonal $CeVO_4$ nanoparticles is 58 nm.
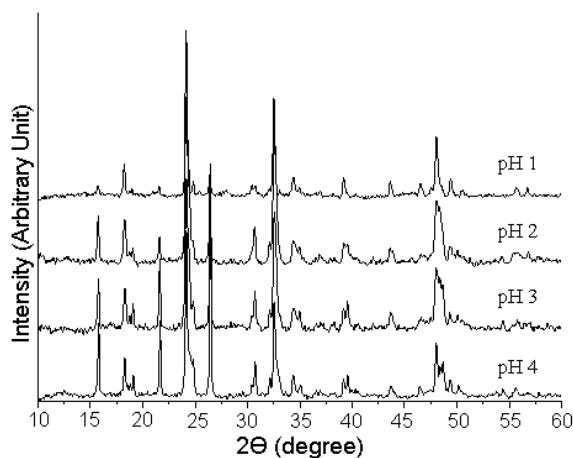


*Fig. 1 XRD patterns of the samples hydrothermally synthesized in the solutions with the pH of 1, 2, 3 and 4.*

Fig. 2 shows the FTIR and Raman spectra of $CeVO_4$ nanoparticles. FTIR spectrum (Fig. 2a) shows a sharp peak at $800\,cm^{-1}$ due to the V–O stretching vibration of $VO_4$ [8, 12, 13]. The broad band at $3,420\,cm^{-1}$ is identified to the O–H stretching of adsorbed water on the surface of $CeVO_4$ [8]. Raman spectrum (Fig. 2b) of $CeVO_4$ shows a strongest peak at $860\ cm^{-1}$ which is assigned to the intra-tetrahedral V–O bonds of symmetric stretching mode ($v_1$) of $A_{1g}$ symmetry. The Raman peaks at 795 and $782\ cm^{-1}$ are assigned to the asymmetric stretching modes ($v_3$) of $E_g$ and $B_{1g}$ of $CeVO_4$. The bending modes of $v_4(B_{1g})$ and $v_2(A_{1g})$ were detected at 466 and $377\ cm^{-1}$, respectively. The Raman peak at $263\ cm^{-1}$ was specified as the $v_2(B_{2g})$ bending mode of the $VO_4$ tetrahedrons [14, 15].
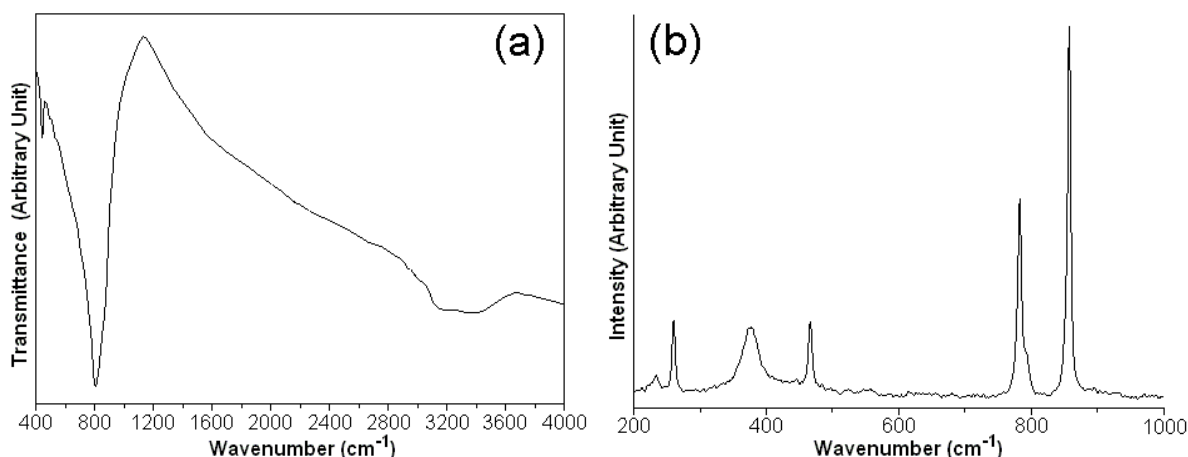


*Fig. 2 (a) FTIR and (b) Raman spectra of $CeVO_4$ sample hydrothermally synthesized in the solution with the pH of 1.*

Fig. 3 shows SEM images with four different magnifications of $CeVO_4$ nanocrystals synthesized by hydrothermal reaction at 200 °C for 24 h. It should be noted that the crystalline product is agglomerated nanoparticles size below 100 nm calculated by using Scherrer equation. In order to decrease their surface energies, the very tiny nanoparticles agglomerated to form larger

ones [16]. Thus less surface particles exist outside. These surface particles are unsaturated and have vacant coordination sites and dangling bonds. They have very high affinity to form bonds with adjacent particles, leading to agglomeration. Thus small particles try to cluster together in groups by forming bonds with nearby particles.
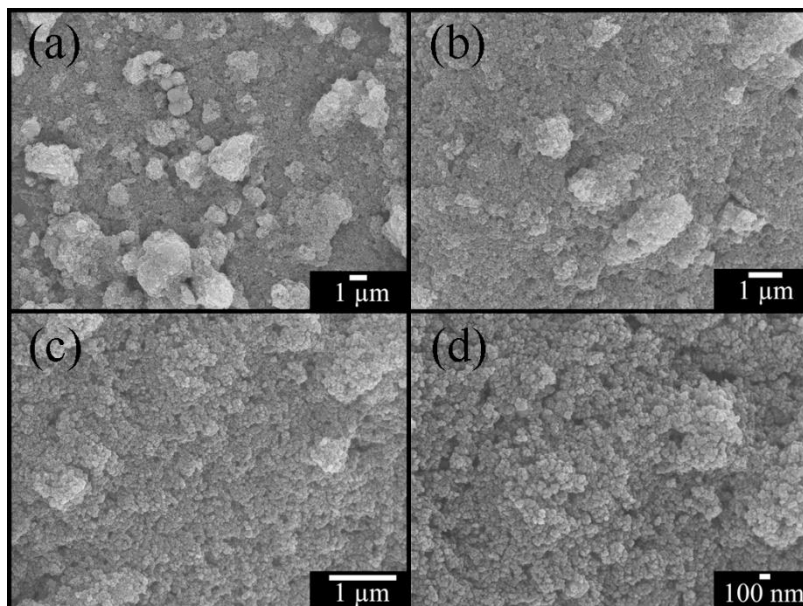


*Fig. 3 SEM images of CeVO$_4$ nanoparticles hydrothermally synthesized in the solution with the pH of 1 at magnification of (a) 5,000X (b) 10,000X (c) 20,000X and (d) 30,000X.*

TEM images and SAED patterns of CeVO4 at pH 1 are shown in Fig. 4. TEM shows that the products were composed of dispersed round nanoparticles with the sizes of 50-100 nm. Their SAED patterns shows a diffuse and hollow concentric rings of bright spots, caused by the diffraction of transmitted electrons through the nanocrystals with different orientations. SAED pattern was indexed to the (101), (200), (112), (220), (301), (103), (312) and (400) planes for tetragonal CeVO$_4$ structure with according to with those of the JCPDS database [9].
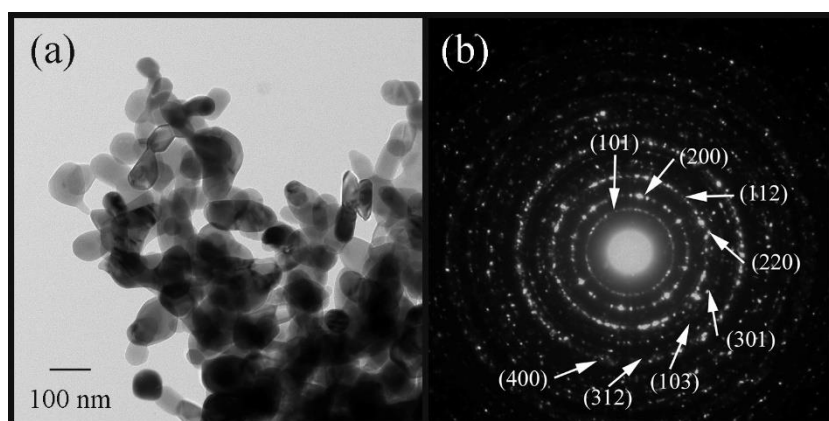


*Fig. 4 TEM image and SAED pattern of CeVO4 nanoparticles*

Fig. 5 shows UV-visible spectra for the degradation of MB by the CeVO$_4$ nanoparticles under UV irradiation for 0–300 min. Clearly, the MB has a maximum visible absorption at 664 nm wavelength. Upon being irradiated by UV, the intensity of MB at 664 nm was decreased with the

increasing in the UV irradiation time, confirmed the photocatalytic degradation of MB by the demethylation process [17, 18] to produce the degradation product.
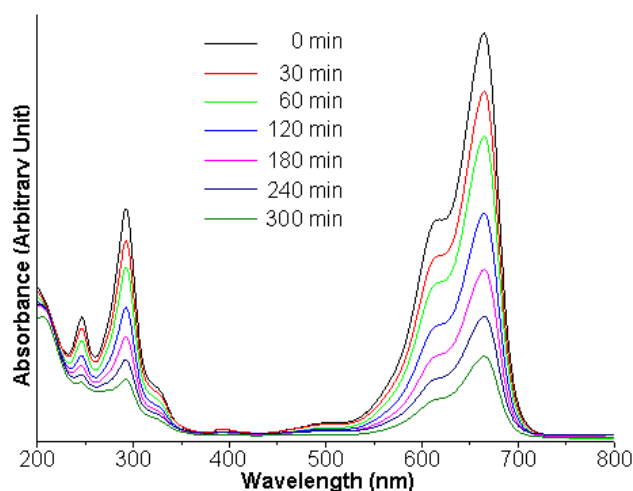


*Fig. 5 UV-visible absorption spectra of MB in the solution containing CeVO$_4$ as a photocatalyst under UV irradiation within 0–300 min.*

The MB degradation using CeVO$_4$ as a photocatalyst under UV irradiation was carried out as the results shown in Fig. 6a. In this research, the MB solution without CeVO$_4$ nanoparticles as a photocatalyst was not degraded under UV irradiation. In the solution containing CeVO$_4$, 80 % of MB was degraded within 300 min UV irradiation. The degradation rate for CeVO$_4$ is shown in Fig. 6b. The photocatalytic degradation reaction is assumed to follow a pseudo-first-order expression

$$\ln(C_o/C_t) = kt \tag{3}$$

where k is the apparent rate constant (min$^{-1}$), C$_o$ is the initial concentration of MB, and C$_t$ is the solution-phase concentration of MB within the elapsed time (t). C$_t$/C$_o$ is the normalized organic compound concentration [8, 17, 19]. The relationship between $\ln(C_o/C_t)$ and t for the photocatalytic degradation reaction of CeVO$_4$ was fitted to a linear regression line with $R^2 = 0.9980$, confirmed the pseudo-first-order reaction photocatalytic degradation. The rate constant for MB degradation by the CeVO$_4$ nanoparticles is $5.5 \times 10^{-3}$ min$^{-1}$. The photocatalytic mechanism for the degradation of MB by CeVO$_4$ as a photocatalyst can be explained as follows [8].

$$CeVO_4 \qquad \rightarrow \qquad e^- + h^+ \tag{4}$$

$$O_2 + e^- \qquad \rightarrow \qquad {}^{\bullet}O_2{}^- \tag{5}$$

$$OH^-/H_2O + h^+ \qquad \rightarrow \qquad {}^{\bullet}OH \tag{6}$$

$$MB + {}^{\bullet}O_2{}^-/{}^{\bullet}OH \quad \rightarrow \quad \text{Decomposed molecules} \tag{7}$$
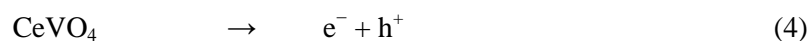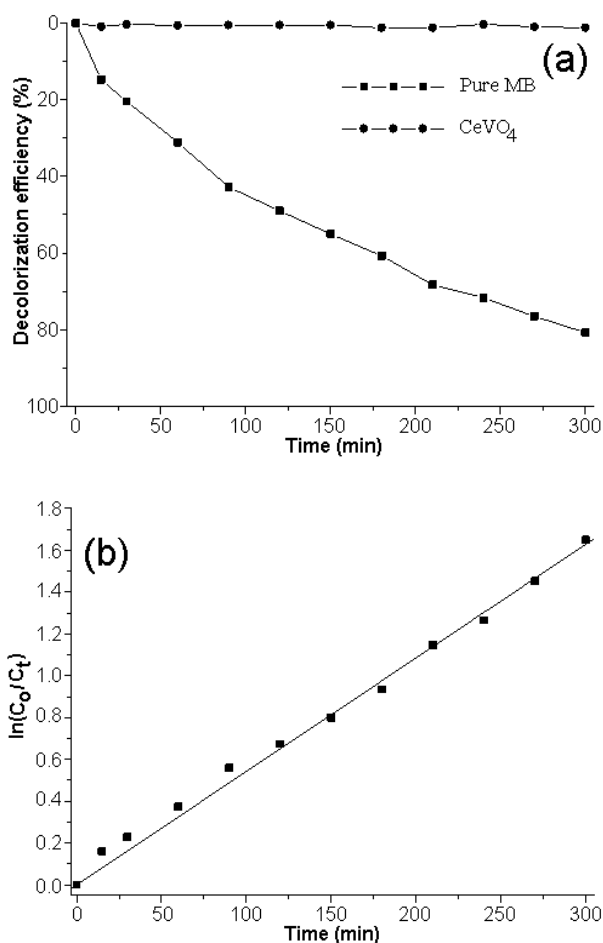
*Fig. 6 (a) Decolorization efficiency of MB by CeVO₄ nanoparticles comparing to that of MB by the blank and (b) the first-order plot for the photocatalytic degradation of MB by CeVO₄ nanoparticles under UV irradiation.*

Under UV irradiation, the CeVO$_4$ nanoparticles as a photocatalyst were excited to form electrons (e$^-$) in conduction band and holes (h$^+$) in valence band. Subsequently, the photoexcited electrons in conduction band of CeVO$_4$ was transferred to the adsorbed O$_2$ on the surface of CeVO$_4$ to form $^\bullet$O$_2^-$ radicals. Concurrently, OH$^-$/H$_2$O ions/molecules were protonated by h$^+$ on valence band of CeVO$_4$ to form $^\bullet$OH radicals. Finally, $^\bullet$O$_2^-$ and $^\bullet$OH radicals attacked the MB molecules to form decomposed molecules, such as CO$_2$ and water.

## 4. Conclusions

In summary, UV-light-induced CeVO$_4$ photocatalyst has been successfully synthesized by hydrothermal method. It show a high efficiency in the degradation of 5 x 10$^{-5}$ M MB of 80 % at the degradation rate of 5.5 $\times$ 10$^{-3}$ min$^{-1}$ within 300 min under UV irradiation. The mechanism of photocatalysis of MB by the CeVO$_4$ nanoparticles was also discussed.

## References

[1] J. Huang, S. Liu, L. Kuang, Y. Zhao, T. Jiang, S. Liu, X. Xu, J. Environmental Sci. **25**, 2487 (2013).

[2] M. Reli, M. Edelmannová, M. Sihor, P. Praus, L. Svoboda, K.K. Mamulová, H. Otoupalíková, L. Capek, A. Hospodková, L. Obalová, K. Koćá, Inter. J.  Hydrogen Energ. **40**, 853 (2015).

[3] J. Tian, Y. Leng, H. Cui, H. Liu, J. Hazard. Mater. **299**, 165 (2015).

[4] S. Shaker-Agjekandy, A. Habibi-Yangjeh, Mater. Sci. Semicon. Proc. **34**, 74 (2015).

[5] P. Chen, Q. Wu, L. Zhang, W. Yao, Catal. Commun. **66**, 6 (2015).

[6] S. Mahapatra, G. Madras, T.N.G. Row, Ind. Eng. Chem. Res. **46**, 1013 (2007).

[7] A.H. Shah, Y. Liu, W. Jin, W. Chen, I. Mehmood, V.T. Nguyen, Mater. Lett. **154**, 144 (2015).

[8] N. Ekthammathat, T. Thongtem, A. Phuruangrat, S. Thongtem, J. Nanomater. **2013**, 1 (2013) Article ID 434197.

[9] Powder Diffract. File, JCPDS Internat. Centre Diffract. Data, PA 19073–3273, U.S.A. (2001).

[10] C. Suryanarayana and M. G. Norton, X-Ray Diffraction: A Practical Approach, Plenum Press, New York, NY, USA, 1998.

[11] A. Phuruangrat, N. Ekthammathat, T. Thongtem, S. Thongtem, J. Phys. Chem. Solids **72**, 176 (2011).

[12] X. Yang, W. Zuo, F. Li, T. Li, Chem. Open **4**, 288 (2015).

[13] G. Çelik, F. Kurtuluş, Acta Phys. Pol. A **125**, 358 (2014).

[14] Y. Shen, Y. Huang, S. Zheng, X. Guo, Z.X. Chen, L. Peng, W. Ding, Inorg. Chem. **50**, 6189 (2011).

[15] R. Rao, A.B.Garg, B.N.Wani, J. Phys. Conf. Ser. **377**, 12010 (2012).

[16] W.S. Chiu, S. Radiman, R. Abd-Shukor, M.H. Abdullah, P.S. Khiew, J. Alloy. Compds. **459**, 291 (2008).

[17] O. Yayapao, T. Thongtem, A. Phuruangrat, S. Thongtem, Mater. Sci. Semicon. Proc. **39**, 786 (2015).

[18] S. Naghizadeh-Alamdari, A. Habibi-Yangjeh, M. Pirhashemi, Solid State Sci. **40**, 111 (2015).

[19] A. Phuruangrat, A. Maneechote, P. Dumrongrojthanath, N. Ekthammathat, S. Thongtem, T. Thongtem, Superlattice. Microst. **78**, 106 (2015).